Available online at www.sciencedirect.com

ScienceDirect

Energy Procedia 38 (2013) 589 – 596

Energy Procedia

SiliconPV: March 25-27, 2013, Hamelin, Germany

Impact of a p-type solar cell process on the electrical quality of Czochralski silicon

Kevin Lauer[a,*], Christian Möller[a,b], Kristin Neckermann[a], Michael Blech[a], Martin Herms[c], Teimuraz Mchedlidze[d], Jörg Weber[d], Sylke Meyer[e]

[a]CiS Forschungsinstitut für Mikrosensorik und Photovoltaik GmbH, Konrad-Zuse-Str. 14, 99099 Erfurt, Germany
[b]TU Ilmenau, Institut für Physik, Weimarer Str. 32, 98693 Ilmenau, Germany
[c]Bosch Solar Energy AG, Robert-Bosch-Str. 1, 99310 Arnstadt, Germany
[d]Technische Universität Dresden, 01062 Dresden, Germany
[e]Fraunhofer-Center für Silizium Photovoltaik CSP, Walter-Hülse-Str. 1, 06120 Halle (Saale), Germany

Abstract

The impact of the three main process steps during p-type solar cell processing, namely phosphorus diffusion, anti-reflection coating and contact formation, on the electrical quality of Cz silicon is investigated. Adjacent wafers from the middle and tail part of three Czochralski grown silicon ingots of varying quality were treated by the process steps as well as process step combinations. The impact of the thermal budget during the process steps without the application of phosphorus dopant, ammonia and silan gases and metal contact pastes on the Cz silicon was examined. The excess charge carrier lifetime and the interstitial iron content were measured separately for each step. Besides other effects, phosphorus diffusion gettering was found to be very efficient in removing interstitial iron from the Cz silicon. The antireflection coating step as well as the contact formation step were found to be most detrimental to the Cz silicon quality. Changes observed in the Cz silicon quality were discussed within the frame of recent models.

Keywords: Cz-silicon, solar cell process, lifetime, iron content

1. Introduction

The thermal budget from diffusion as well as coating steps during the solar cell process affects the electrical quality of Czochralski grown silicon. In contrast to multicrystalline silicon, where knowledge

*Corresponding author. Tel.: -49 361 663 1211; fax: +49 361 663 1413.
E-mail address: klauer@cismst.de.

doi:10.1016/j.egypro.2013.07.321

exists [1] about the dominant physical mechanism controlling the electrical quality during the solar cell fabrication, the impact of the solar cell process on Cz silicon is only poorly investigated. The different quality of Cz silicon compared to multicrystalline silicon results in a different response to the solar cell process steps. An understanding of the physical processes in Cz silicon during the solar cell process is necessary to improve the process steps and in consequence to improve the performance of p- as well as of n-type Cz silicon solar cells.

Starting from differently contaminated Cz silicon, the present work investigates the impact of process steps during p-type solar cell fabrication on the electrical quality of Cz silicon. Changes in the excess charge carrier lifetime as well as in the interstitial iron content are monitored for different process steps as well as process sequences.

2. Experimental

2.1. Samples

The samples investigated in this study originate from three Czochralski crystals (groups are labeled A, B and C), which were grown at Bosch Solar Energy AG. For each run the quality of the silicon feedstock was varied. An overview of the iron content measured in the feedstock and in the crystal is given in Tab. 1. The interstitial iron contamination level determined by lifetime measurements in the samples ranges from ~5×10^{11}cm^{-3} for group C to ~5×10^{10}cm^{-3} for group A. In group B the interstitial iron content lies below the detection limit of 10^{10}cm^{-3}. The crystals were boron doped to reach a specific resistivity in the range of 3 Ωcm < ρ_s < 6 Ωcm. After sawing of the crystals, wafers were taken for the investigation from the top and bottom part of the ingot. Additionally, floating zone silicon samples grown from electronic grade silicon were used as reference material.

Table 1. Overview of iron content measured by different methods in the feedstock and in the crystal of samples A, B and C. Measurements were done near the center of the wafer.

sample		ICPMS, feedstock [Fe] [cm^{-3}]	ICPMS, crystal [Fe] [cm^{-3}]	Lifetime, crystal [Fe_i] [cm^{-3}]	DLTS, crystal [Fe_i/FeB] [cm^{-3}]
A	top	$(4.2\pm0.3)\times10^{13}$	$(3.8\pm0.3)\times10^{13}$	$(4.0\pm1.0)\times10^{10}$	$<2\times10^{11}$
	tail		$(9.9\pm1.4)\times10^{13}$	$(5.8\pm0.9)\times10^{10}$	
B	top	$(6.5\pm1.3)\times10^{13}$	$(2.9\pm2.9)\times10^{13}$	$<10^{10}$	$<1\times10^{11}$
	tail		$<2.9\times10^{13}$	$<10^{10}$	
C	top	$(2.0\pm1.2)\times10^{14}$	$(9.1\pm9.1)\times10^{14}$	$(2.7\pm0.5)\times10^{11}$	$<3\times10^{11}$
	tail		$<2.8\times10^{13}$	$(8.2\pm0.3)\times10^{11}$	

2.2. Process

The temperature-time-profile of the p-type solar cell process [2], which was applied to the Cz silicon wafers, is depicted in Fig. 1. Two process runs were performed. In the first run group A was processed and in the second run group B, C and partially a FZ reference group (FZ1) were processed. After etching off the saw damage by KOH solution and RCA cleaning of adjacent wafers different process steps were applied alone as well as in combination. The individual process steps were phosphorus diffusion, anti-reflection coating and contact formation. Phosphorus diffusion (abbreviated as P) was done in a walking string inline furnace. The phosphorus dopant was deposited by spray coating of phosphoric acid solution.

To simulate the impact of the annealing temperature during phosphorus diffusion on the silicon the spray-on doping was omitted for several process groups (abbreviated with SP). Coating of the anti-reflection SiN_x-layer was done using a PECVD reactor (abbreviated as AR). In case of the simulation step (SAR) the process gases (silan and ammonia) were omitted and the annealing step was done in the PECVD reactor under argon atmosphere. Contacts (C) were formed in a two step process by screen printing of silver paste on the front side and aluminium paste on the back side with a subsequent low temperature drying step. In the second step, the samples were annealed in a sintering furnace. For simulation of the annealing step during contact formation (SC), the pastes were omitted before annealing in the sintering furnace.

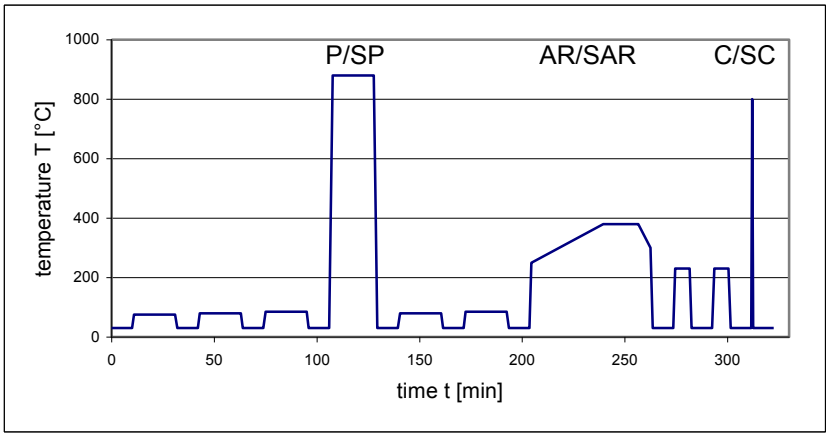

Fig. 1. Temperature as a function of time for the solar cell process, which has been applied to the Cz silicon material. The phosphorus diffusion, anti-reflection coating and sintering step are denoted by P, AR and C, respectively. The addition of S (simulation) means that only the temperature of this step impacts the Cz silicon. Dopants, process gases and metal pastes (silver front side, aluminum backside) are omitted in this case.

After processing the wafers were quartered. One quarter was used for lifetime as well as interstitial iron analysis. All layers on top of the quarter wafers (phosphorus diffused region, silicon nitride coating, metal pastes and aluminium diffused region) were removed by various etching solutions. Complete removal of the doping layers was checked by specific resistance measurements.

2.3. Measurement methods

For the purpose of measuring the excess charge carrier lifetime of the bulk silicon, the recombination at the silicon surfaces is minimized by coating the wafer surface with silicon nitride [3]. The carrier lifetime is measured using the RF-PCD setup from Sinton Consulting Inc. [4]. The interstitial iron content is determined from the carrier lifetime in both states of the meta-stable iron-boron-pair complex and evaluated regarding the Shockley-Read-Hall (SRH) statistics [5, 6]. The parameters of the SRH recombination statistics for interstitial iron as well as iron boron pairs are taken from Refs. [7, 8], respectively. The carrier lifetime before dissociation of the iron boron pairs is given in the diagrams. Measurements are done at four positions per wafer. The error bars represent the standard deviation between these four measurements.

DLTS measurements were performed by means of a standard lock-in system working at the capacitance testing frequency of 1 MHz. Principles of the method and the system were previously

described [9]. Cooling of a sample was done by immersion in a dewar with liquid He, and a temperature controller maintained the necessary temperature in the range of 35-300 K. Samples were protected from non-equilibrium illumination during the measurements.

For the DLTS measurements, the solar cell structure was removed from the surface of the solar cells by an etching to the depth of 50 µm and an Al film was deposited for Schottky contacts. The Ohmic contacts were made by rubbing an InGa alloy into the back surface of the samples.

ICPMS analyses were performed after complete chemical digestion of about 1 g of the corresponding silicon sample using a high resolution ICP mass spectrometer.

3. Results and discussion

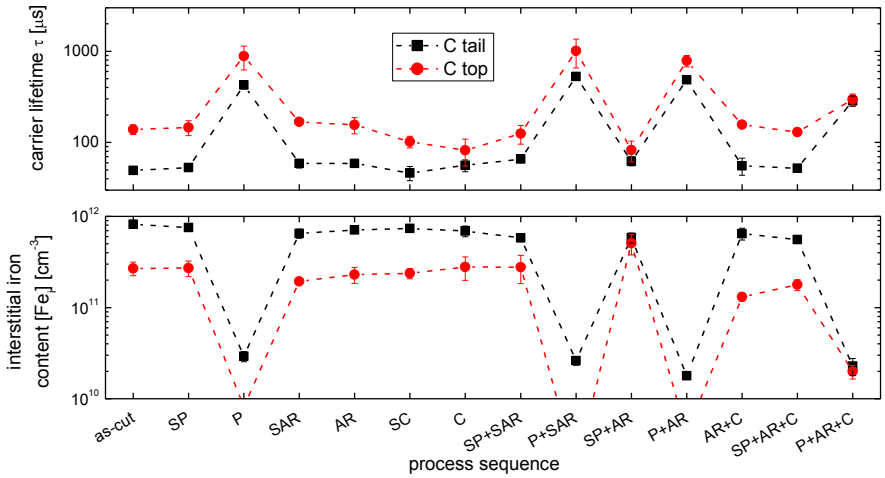

Fig. 2. Lifetime and interstitial iron content of all investigated processes and process sequences for group C. The difference in lifetime and interstitial iron content between top and tail is visible for all process sequences except for the completely fabricated solar cell (P+AR+C).

The results of the lifetime and interstitial iron measurements are exemplarily depicted in Fig. 2 for group C. The difference in lifetime and interstitial iron content between top and tail of the crystal is visible for all process sequences except for the completely fabricated solar cell (P+AR+C). But there is no significantly different response of the top and tail samples to the process sequences. Hence, for the following detailed analysis of the impact of the process sequences on the Cz silicon, the average of the top and tail lifetime as well as interstitial iron content is used.

3.1. Phosphorus diffusion

The lifetime as well as the interstitial iron content determined after different process sequences, which include the phosphorus diffusion step (P and SP), are depicted in Fig. 3. The lines between two measurement points visualize the impact of the phosphorus doping. The annealing step (SP) decreases the lifetime and increases the interstitial iron content slightly for groups A, B and the Fz reference (FZ1). In group C both quantities do not change significantly. There are two possible explanations for the changes in groups A and B. First, during the high temperature anneal, iron precipitates were dissolved leading to a

lower lifetime and increased interstitial iron content. This is plausible as ICPMS measurements detected considerable iron concentrations in all three groups (see Tab. 1). Second, there could be a contamination of the samples either by cross contamination from the highly contaminated group C or by the furnace atmosphere. The first thesis is supported as the Fz reference samples (FZ1) processed in the same run as groups B and C were degraded, too. Contamination by furnace atmosphere can be excluded by looking at the second Fz reference (FZ2). This group was processed solely. Hence, cross contamination from other samples could not take place. Group FZ2 was not degraded during the phosphorus diffusion anneal (SP). Thus, the increase in the interstitial iron content in group A can be explained by dissolution of iron precipitates. However, the increase in the interstitial iron content in groups B and FZ1 is most probably caused by cross contamination during processing from group C.

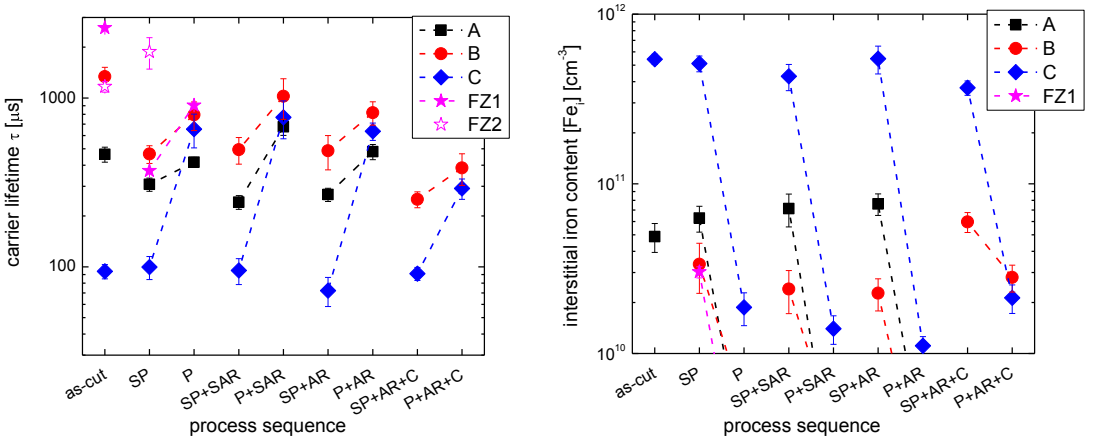

Fig. 3. Lifetime and interstitial iron content measured after different process sequences including the phosphorus diffusion step with (P) and without (SP) phosphorus spray-on dopant. The lines between two measurement points visualize the impact of the phosphorus doping.

The beneficial impact of the phosphorus diffusion gettering [10] is visible in Fig. 3 for all process sequences, which include SP and P. By adding phosphorus, the lifetime increases and the interstitial iron content decreases drastically, in particular for group C. It is found by comparing the measured lifetime for the process sequences P and P+SAR that the phosphorus gettering is further enhanced in combination with SAR.

3.2. Antireflection coating

Figure 4 shows the lifetime and the interstitial iron content with regard to the antireflection coating step. The lines between two measurement points visualize the impact of the process gases and in consequence the impact of the silicon nitride layer. The interpretation of the results is complicated by the fact that the surface passivation process applied to suppress surface recombination is nearly the same as the AR step. Hence, the AR annealing step is applied two times for the as-cut samples and three times for the AR and SAR samples. It is improbable that the decrease in lifetime found for the SAR and AR samples in comparison to the as-cut sample is caused by the thermal budget. Probably, the cleaning by a shortened RCA after KOH etching, which was applied only to the SAR and AR samples, was not

sufficient to remove all surface contaminants. All other groups have seen a complete RCA cleaning after KOH etching. Nevertheless, in comparison to the as-cut samples the interstitial iron content decreases in groups A and C due to the SAR and AR step. This effect can be explained by low temperature precipitation of interstitial iron [11].

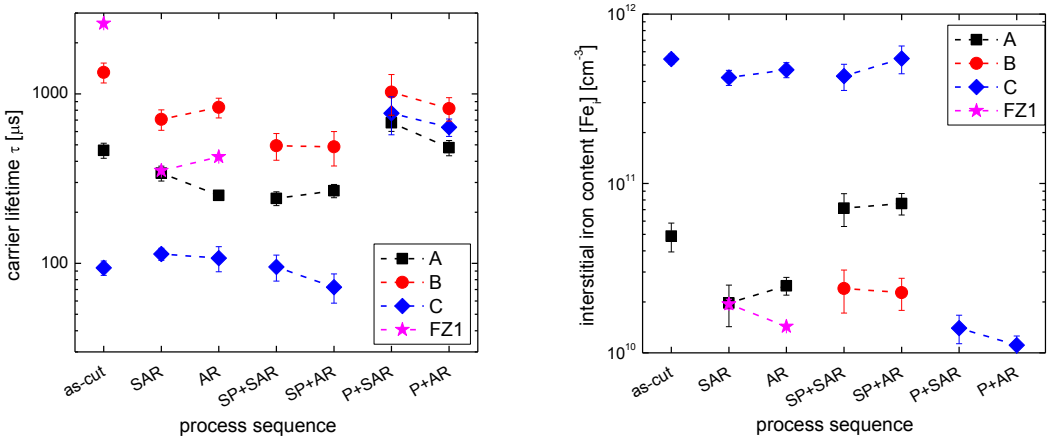

Fig. 4. Lifetime and interstitial iron content measured for the groups A, B and C after different process sequences including the anti-reflection coating step with (AR) and without (SAR) process gases. The lines between two measurement points visualize the impact of the process gas.

Interestingly, a detrimental impact of the process gases and the silicon nitride layer on Cz silicon is found if the P+SAR and P+AR process sequences are compared. This is in contrast to multicrystalline silicon, where hydrogen supplied by the process gases in the AR step passivates bulk defects like dislocations and grain boundaries. A beneficial effect of hydrogen on the silicon bulk properties of Cz silicon could not be observed. It is known that nitridation reduces the silicon interstitial concentration during dopant diffusion [12]. Possibly, the vacancy injection due to tensile stress induced by the formation of the silicon nitride layer is responsible for the lifetime degradation, which is observed by comparing the P+SAR and P+AR step.

3.3. Contact formation

The lifetime as well as the interstitial iron content with regard to the contact formation step is shown in Fig. 5. The lifetime decreases after sintering with (C) and without (SC) pastes compared to the as-cut values of groups B, C and FZ1. This can be explained by contamination from the furnace atmosphere as there are no protecting layers like P-diffused regions or aluminum pastes for the SC samples. Another explanation for the degradation of groups B and FZ1 is again the cross contamination by group C.

In the case of the samples with screen printed pastes, there is one diffusion barrier due to the aluminum paste on the backside. However, there is no clear trend regarding the lifetime change with (C) and without (SC) pastes.

Besides the protecting layers, which impact the Cz silicon, aluminum gettering should have a beneficial impact on the silicon. This effect is only visible in one case. For the highly contaminated group C a reduction of the interstitial iron content due to the contact formation step (C) is found if the high

temperature annealing step (SP) and silicon nitride layer (AR) is applied (comparing SP+AR and SP+AR+C). In the other cases, the application of the pastes and the contact formation step does not reduce the interstitial iron content. The interstitial iron content even increases comparing the SC and C step of group B and FZ1. Hence, there is a contamination of the silicon due to the pastes. By comparing SP+AR and SP+AR+C for group B and P+AR and P+AR+C for groups B and C, a decrease in lifetime and an increase in the interstitial iron content is found.

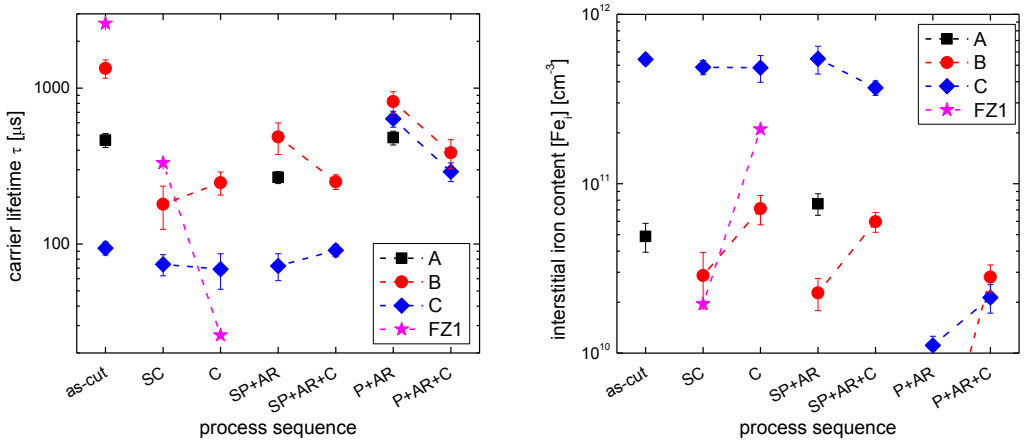

Fig. 5. Lifetime and interstitial iron content measured for the groups A, B, C and FZ1 after different process sequences including the contact formation step with (C) and without (SC) contact pastes.

3.4. Results of DLTS measurements

Excluding the near-edge (< 15 mm) regions of the wafers, the carrier traps were detected at several locations of the bulk material in the as-cut and processed wafers from the A crystal. Most frequently a majority carrier trap with energy level position at $E_t = E_V + 0.42$ eV and apparent capture cross-section $\sigma = 5\times10^{-18}$ cm^{-2} was detected. The DLTS signal revealed logarithmic dependence of its amplitude on the filling pulse length and, thus, the related trap should be attributed to extended defects (e.g. to dislocations or to oxide precipitates). The trap density reached ~10^{12} cm^{-3} for some locations. Another majority carrier trap with parameters $E_t = E_V + 0.27$ eV and apparent capture cross-section $\sigma = 3\times10^{-18}$ cm^{-2} was detected less frequently. The trap was also related to extended defects and the maximal density detected was 3×10^{11} cm^{-3}. In the fully processed solar cells, after removal of solar cell structure, similar traps were detected without significant variations in concentration. It should be explicitly stated that DLTS signals related to interstitial iron or to FeB complexes were below the detection limit of the method ($<2\times10^{11}$ cm^{-3}) for all locations except the near-edge region of the wafers.

4. Summary

Czochralski silicon wafers from three different crystals were investigated with respect to changes in electrical quality during p-type solar cell processing. The excess charge carrier lifetime as well as the interstitial iron content were measured after the three main steps of the p-type solar cell process as well as

after several combinations of these process steps. The steps are the phosphorus diffusion, the anti-reflection coating and the contact formation. The three starting groups of Cz silicon wafers varied in lifetime as well as in the interstitial iron content.

The key findings of this investigation were as follows. Phosphorus diffusion gettering was very efficient in increasing the lifetime and reducing the interstitial iron content. The interstitial iron content was reduced for all processes including the P-diffusion by more than one order of magnitude. For the group, which exhibited medium interstitial iron contamination of about $\sim 5\times10^{10}cm^{-3}$, dissolution of iron precipitates during the diffusion annealing step was visible. It was found that simultaneous processing of highly ($[Fe_i]\sim 5\times10^{11}cm^{-3}$) and non-contaminated samples led to a contamination of the initially non-contaminated samples. A beneficial effect of hydrogen supplied during the anti-reflection coating as known for multicrystalline silicon was not observed for Cz silicon. On the contrary, the application of the silicon nitride layer on the phosphorus diffused region led to a significant reduction in the lifetime for all groups. We explained this by a defect formation in the Cz silicon due to vacancy injection during the anti-reflection coating step. Vacancies are generated due to the tensile strain induced by the silicon nitride layer. It was found that the thermal budget of the anti-reflection coating step leads to low temperature iron precipitation and thus reduces the interstitial iron content. The contact formation step was in most cases detrimental to the lifetime. A contamination with iron by the metal pastes was observed. For the highly iron contaminated group, the interstitial iron content was reduced in one case by application of the contact formation step. This effect was explained by aluminum gettering of iron.

Acknowledgements

The authors gratefully acknowledge the financial support by the German Federal Ministry of Education and Research within the framework of the Leading-Edge Cluster Competition and the research cluster Solarvalley Central Germany under contract No. 03SF0398A (xμ-Material).

References

[1] A. Cuevas, D. MacDonald, “Multicrystalline Silicon: a Review of Its Electronic Properties”, PVSEC 2005, Shanghai Scientific & Technological Literature Publishing House, Shanghai, pp. 521-524.

[2] J. Szlufcik, F. Duerinckx, E. van Kerschaver, R. Einhaus, A. Ziebakowski, E. Vazsonyi, K. D. Clercq, J. Horzel, L. Frisson, J. Nijs, R. Mertens, Proc. 14th European Photovoltaic Solar Energy Conference, WIP-Munich, Germany (1997) 380

[3] A. Laades, M. Blech, M. Bähr, K. Lauer, and A. Lawerenz, Phys. Stat. Solidi C **8**, 763-766 (2011)

[4] R. Sinton, A. Cuevas, Appl. Phys. Lett. **69** (1996) 2510

[5] W. Shockley and W. Read, Phys. Rev. **87** (1952) 835

[6] R. N. Hall, Phys. Rev. **87** (1952) 387

[7] A. A. Istratov, H. Hieslmair, and E. R. Weber, Appl. Phys. A: Mater. Sci. Process. **69** (1999) 13

[8] S. Rein and S. Glunz, J. Appl. Phys. **98** (2005) 113711

[9] G. L. Miller. D. V. Lang. and L. C. Kimerling, Ann. Rev. Mater. Sci. 7 (1977) 377

[10] S. M. Myers, M. Seibt and W. Schröter, J. Appl. Phys. **88** (2000) 3795

[11] W. B. Henley, D. A. Ramappa, J. Appl. Phys. **82** (1997) 589

[12] A. Ural, P. B. Griffin and J. D. Plummer, J. Appl. Phys. **85** (1999) 6440